

Solution of the Nucleon Structure Problem from a Field Theory of Fermions and Bosons and the Origin of the Proton Stability

Hans-Peter Morsch 

HOFF, Jülich, Germany

Email: h.p.morsch@gmx.de

How to cite this paper: Morsch, H.-P. (2024) Solution of the Nucleon Structure Problem from a Field Theory of Fermions and Bosons and the Origin of the Proton Stability. *Journal of High Energy Physics, Gravitation and Cosmology*, 10, 1655-1669. <https://doi.org/10.4236/jhepgc.2024.104093>

Received: June 9, 2024

Accepted: October 9, 2024

Published: October 12, 2024

Copyright © 2024 by author(s) and Scientific Research Publishing Inc. This work is licensed under the Creative Commons Attribution International License (CC BY 4.0).

<http://creativecommons.org/licenses/by/4.0/>



Open Access

Abstract

A bound state formalism derived from a fermion-boson symmetric Lagrangian has been used to calculate the nucleon masses, the charge neutrality of the neutron, the magnetic moments and the electromagnetic form factor ratios $\mu_p G_{E_p} / G_{M_p}$ and $\mu_n G_{E_n} / G_{M_n}$. A quantitative description is obtained, assuming a mixing of a scalar bound state of $3(f \bar{f})f$ structure with its corresponding vector $(f \bar{f})f$ state (f indicating massless elementary fermions). Only a few parameters are needed, mainly fixed by energy and momentum conservation. The nucleon stability is explained by an extra binding in the confinement potential, negative for electric and positive for magnetic binding of the proton, and opposite for the neutron. The stronger electric extra binding of the proton allows a decay of the neutron to proton and electron.

Keywords

Proton and Neutron Properties Described in a New Bound State Formalism by a Mixing of Two Related Bound States, Quantitative Agreement with Their Masses, Radii, Magnetic Moments and Electromagnetic Form Factor Ratios, High Stability Due to Extra Binding in the Confinement Potential

1. Introduction

Without the existence of stable protons composite particles like nuclei, atoms and molecules, but also the full complexity of nature could not have been developed. Therefore, there is a deep interest to understand the nucleon structure, in particular the origin of its stability. During the last decades large experimental and theoretical efforts have been made to understand this problem. Experimentally, large

sets of data have been taken on hadron and lepton scattering and reactions. In comparison to hadrons, more detailed and reliable information has been expected from electromagnetic probes [1]. Therefore, data on electromagnetic form factors have been collected up to large momentum transfers in electron scattering from the proton [2]-[7] and neutron [8]-[11].

Concerning the properties of nucleons, the proton has an exponentially falling charge density with a root mean square radius of about 1 fm, whereas the neutron has a vanishing charge density (integrated over full space) with regions of radius of positive and negative charge. Further, nucleons have a magnetic dipole moment, $M1 = 2.793$ for the protons and 1.913 for the neutron, which has given early evidence that nucleons are complex objects.

The root mean square radius of the charge density of the proton has been determined from electron scattering and lamb shifts in muonic hydrogen to be about 0.88 fm, but later revised to 0.84 fm [12]. But the electron form factors measured up to large momentum transfers could suggest an even smaller proton radius. A rather small radius has been deduced also from 4 GeV α - p scattering [MSD], but with larger uncertainties due to strong absorption effects. Another interesting fact, in an early empirical analysis of its electromagnetic structure by Kelly [13], it has been found that the charge and magnetization densities of the proton should be different. This has been nicely confirmed by polarization experiments of electromagnetic form factors [14] [15], but up to date this observation has never been satisfactorily explained.

Theoretically, the nucleon problem has been studied during decades in many different models and was subject of numerous conferences and specialized workshops. Its structure has been discussed in several versions of the quark model [16] [17], in various Bag models [18] [19], in descriptions inspired from quantum chromodynamics, see ref. [20], by using the Dyson-Schwinger equation [21], and in many empirical approaches. In particular, the confinement problem has not been understood [22]-[24] as well as the question of the enormous stability of the proton. In the flux-tube model [25] [26] it was assumed that interacting coloured bosons (gluons) form a plasma, by which the fermions are firmly confined, whereas in string models [27] the fermions should be bound by boson strings.

Significant progress in the understanding of particle properties has been made within the Standard Model of particle physics, see e.g. ref. [20], which is composed of gauge invariant quantum theories of electromagnetic, strong and weak interactions. In particular, quantum chromodynamics, its strong interaction part, has been expected to be well suited for the description of the nucleon. Calculations on the proton have been performed on the lattice by adjusting several parameters, but without considering its important electromagnetic structure. A complete calculation of all nucleon properties, including magnetic moments or form factors is not possible, because in this model the radial degree of freedom is not developed explicitly. Therefore, more recent work on nucleon properties has been based on empirical descriptions, see e.g. [28].

During the last decade, an alternative bound state formalism has been developed, based on a quantum field theory, in which in addition to fermions also boson fields have been introduced [Mo1]. This formalism [Mo2] satisfies relativity explicitly, because it contains the space (time) degree of freedom. In addition, it has very few parameters—determined all by basic conservation laws—and has been applied successfully to hadrons and atoms, but also to leptons and gravitational systems [Mo1-Mo6]. If also a quantitative description of the properties of nucleons can be achieved, this should give clear answers, why the proton is stable.

2. Theoretical Description

The underlying Lagrangian may be written in the form

$$\mathcal{L} = \frac{1}{\tilde{m}^2} (\bar{\Psi} D_\nu) i \gamma^\mu D_\mu (D^\nu \Psi) - \frac{1}{4} F_{\mu\nu} F^{\mu\nu} \quad (1)$$

where \tilde{m} is the mass parameter and Ψ are fermion fields, $\Psi = \Psi^+, \Psi^-$. Further, vector boson fields A_μ with coupling g between the fermions are contained in the covariant derivatives $D_\mu = \partial_\mu - igA_\mu$. The second term of the Lagrangian represents the Maxwell term with Abelian field strength tensors $F^{\mu\nu}$ given by $F^{\mu\nu} = \partial^\mu A^\nu - \partial^\nu A^\mu$, which gives rise to both electric and magnetic coupling.

From this Lagrangian a bound state formalism can be deduced by calculating matrix elements $\mathcal{M}(q) \sim \tilde{\mathcal{L}}_1(q) \mathcal{L}_1(q)$ in momentum space, in which the product of the overlapping fermion and boson fields Ψ and A_μ are replaced by dimensionless wave functions $\psi(q)$ and $w(q)$ —which can be considered as the square root of their normalized probabilities in momentum space. For nucleons the fermion wave functions are given by $\psi(q) \sim \frac{1}{\tilde{m}^{9/2}} (\bar{\Psi} \Psi) \Psi$. The boson wave functions are given by $w(q) \sim \frac{1}{\tilde{m}^2} A_\mu A^\nu$, but one pair of boson fields has to be considered as interaction of vector structure $v_\nu(q) = \pm \alpha \frac{1}{\tilde{m}} A_\mu A^\nu$, acting between fermions and between bosons. The complete formalism is discussed in refs. [Mo1, Mo2] and can be applied to hadrons, leptons, atoms, but also to gravitational bound states.

Assuming spherical symmetric systems, the wave functions can be transformed to normal (r, θ, Φ) space by Fourier transformation $\phi(r) = 2\pi \int q^2 dq j_o(qr) \phi(q)$, where $j_o(qr) = \sin(qr)/(qr)$ and $\phi(q, r)$ are fermion or boson wave functions.

Important to point out that for any basic bound state system there are always two fermion and boson wave functions $\psi_{s,v}(r)$ and $w_{s,v}(r)$ of scalar and vector structure (with scalar and vector coupling between their constituents) and of similar radial structure

$$\psi_{s,v}(r) \sim w_{s,v}(r). \quad (2)$$

Since the integration of fermions and bosons goes over 3-dim. and 2-dim. space, respectively, this yields normalization conditions

$$4\pi \int r^2 dr \psi_{s,v}^2(r) = 2\pi \int r dr w_{s,v}^2(r) = 1.$$

The form of the boson wave function of the scalar state is given by

$$w_s(r) = w_{s_0} \exp\left\{-\left(r/b\right)^\kappa\right\}, \quad (3)$$

whereas that of the vector state is given by

$$w_v(r) = w_{v_0} \left[w_s(r) + \beta R \frac{dw_s(r)}{dr} \right]. \quad (4)$$

The factors w_{s_0} and w_{v_0} are obtained from the normalization (see above), whereas βR is given by $\beta R = -\int r^2 dr w_s(r) / \int r^2 dr [dw_s(r)/dr]$, so that both states are orthogonal, with the condition $\int r dr w_s(r) w_v(r) = 0$.

The reasons, why the same form of wave functions is needed for very different systems, is due to two facts: first a geometric constraint

$$\int dr' w_v(r') v_v(r-r') w_v(r') \sim w_s^2(r), \quad (5)$$

second, due to the two and three-dimensional structure of bosons and fermions in Equation (2).

Fermion binding energies are given for N_f fermion bound states by matrix elements of the form

$$E_{ng}^{s,v} = 4\pi N_f \int r^2 dr \psi_{s,v}(r) V_{ng}^{s,v}(r) \psi_{s,v}(r), \quad (6)$$

with two boson potentials for $n = 2, 3$

$$V_{2g}^{s,v}(r) = \frac{\alpha(2s+1)(\hbar c)^2}{8\tilde{m}} \left(\frac{d^2 w_s(r)}{dr^2} + \frac{2}{r} \frac{dw_s(r)}{dr} \right) \frac{1}{w_s(r)} + V_o \quad (7)$$

with $s = 0$ for scalar and $s = 1$ for vector states and

$$V_{3g}^{s,v}(r) = \frac{\alpha^2(\hbar c)}{\tilde{m}} \int dr' w_{s,v}(r') v_v(r-r') w_{s,v}(r'), \quad (8)$$

with an interaction $v_v(r) = -\alpha(\hbar c) w_v(r)$ for $w_v(r) \geq 0$ and $v_v(r) = 0$ for $w_v(r) < 0$.

The potential $V_{2g}^{s,v}(r)$ can be identified with the ‘‘confinement’’ potential (with a quite linear shape towards large radii), needed in meson spectroscopy [22]-[24]. V_o is a small constant, see ref. [Mo2], which may be related to a binding of bosons in the vacuum. The potential $V_{3g}^{s,v}(r)$ represents a boson-exchange potential.

Kinetic energies are given by

$$T_{ng}^{s,v} = \frac{4\pi}{2} \int r^3 dr \psi_{s,v}(r) V_{ng}^{Ts,v}(r) \frac{d\psi_{s,v}(r)}{dr} \quad (9)$$

with

$$V_{1g}^{Ts,v}(r) = \frac{\alpha(2s+1)(\hbar c)^3}{4\tilde{m}^2} \left(\frac{d^2 w_s(r)}{dr^2} + \frac{2}{r} \frac{dw_s(r)}{dr} \right), \quad (10)$$

where $x = 1, 3$ for scalar and vector state, respectively, and

$$V_{2g}^{Ts,v}(r) = \frac{\alpha^2(\hbar c)^2}{\tilde{m}} w_{s,v}(r) w_{s,v}(r). \quad (11)$$

In addition, there is an energy of acceleration of the form

$$\Delta E^{s,v} = \frac{4\pi}{2} \alpha (\hbar c) \int r^4 dr \psi_{s,v}(r) w_{s,v}(r) \frac{d^2 \psi_{s,v}(r)}{dr^2}. \quad (12)$$

In simple hadronic systems, as discussed in ref. [Mo2], this term corresponds to spurious motion and does not contribute to the mass. But in complex systems, as the present one, the total binding energy is given by

$$M_{s,v} = -[E_{ng}^{s,v} + T_{ng}^{s,v} + \Delta E^{s,v}]. \quad (13)$$

In addition to the fermion contributions there are boson matrix elements, leading to energies

$$E_g^{s,v} = 2\pi \alpha^2 N_g \int r dr w_{s,v}(r) v_v(r) w_{s,v}(r), \quad (14)$$

kinetic energies

$$T_g^{s,v} = 2\pi \frac{\alpha^2 (\hbar c)}{4} \int r^2 dr w_{s,v}(r) \frac{1}{r} \frac{dw_{s,v}(r)}{dr} \quad (15)$$

and a contribution from acceleration

$$\Delta E_g^{s,v} = 2\pi \frac{\alpha^2 (\hbar c)}{8} \int r^2 dr w_{s,v}(r) \frac{d^2 w_{s,v}(r)}{dr^2}. \quad (16)$$

Then, the total boson energy is

$$E_{g,tot}^{s,v} = E_g^{s,v} + T_g^{s,v} + \Delta E_g^{s,v}. \quad (17)$$

Important to note, the total fermion and boson energy of particles has to cancel each other, $E_{f,tot} + E_{g,tot} = 0$, see ref. [Mo2], which indicates a coupling to the vacuum.

In the above formalism there are only three parameters for electric binding, the shape and slope parameters κ and b and the coupling constant α . For magnetic bound states there is another parameter, a relative velocity factor (v/c). It turned out that for all systems studied $\kappa = 1.375$ and $\alpha = 2.158$ lead to optimal results. The remaining parameters b and (v/c) are well determined by energy and momentum conservation for scalar and vector states

$$\left[\langle q_f^2 \rangle^{1/2} - \langle q_g^2 \rangle^{1/2} \right] (v/c) \sim (E_{f,tot} + E_{g,tot}), \quad (18)$$

where $\langle q_f^2 \rangle^{1/2} = \left[\int q^4 dq \mathcal{M}_{3g}(q) / \int q^2 dq \mathcal{M}_{3g}(q) \right]^{1/2}$ is the root square momentum of fermions and $\langle q_g^2 \rangle^{1/2} = \left[\int q^3 dq \mathcal{M}^g(q) / \int q dq \mathcal{M}^g(q) \right]^{1/2}$ that of bosons. The matrix elements $\mathcal{M}_{3g}(q)$ and $\mathcal{M}^g(q)$ are the Fourier transformed values of $M_{3g}(r) = 4\pi N V_{3g}(r) \psi^2(r)$ and $M^g(r) = 2\pi N v_v(r) w^2(r)$.

Since $\langle q_f^2 \rangle^{1/2}$ and $\langle q_g^2 \rangle^{1/2}$ are different, the energies have to be modified by recoil corrections $rec = \mp f_{rec} \left(\langle q_f^2 \rangle^{1/2} - \langle q_g^2 \rangle^{1/2} \right) / \left(\langle q_f^2 \rangle^{1/2} + \langle q_g^2 \rangle^{1/2} \right)$, with sign negative for fermions and positive for bosons. Because we are dealing here with two states, we simply use $E_f^{corr} = (1 - f'_{rec}) E_f$ and $E_g^{corr} = (1 + f'_{rec}) E_g$ with f'_{rec} ad-

justed separately to scalar and vector states.

An additional constraint is provided by a mass-radius condition, which is given by

$$Rat_{2g} = \frac{(\hbar c)^2 (v/c)^2}{\tilde{m}(M_s/2)\langle r_{gs}^2 \rangle} = 1. \quad (19)$$

Interestingly, full relativity is automatically included in the present formalism: the mean momentum is equal to the mass, see Equation (18), and consequently the Fourier transformation of the momentum yields a correlation between space and time. The validity of space-time is also directly evident from the mass-radius condition (19).

3. Description of the Nucleon

For systems with a mass of about 0.94 GeV simple $(f \bar{f})f$ bound state solutions¹ as those discussed in ref. [Mo2] do not exist, because energy-momentum conservation is not fulfilled. Further, the measured electromagnetic form factors of proton and neutron are different, which suggests a mixing of states. Since in the present formalism the mass of the vector state M_v is slightly higher than three times the mass M_s of the scalar state, a mixing of a scalar $3 \cdot (f \bar{f})f$ bound state with a vector $(f \bar{f})f$ state (with quite comparable masses) appears to be realistic. Writing the densities in the form $\rho_s(r) = \psi_s^2(r)$ and $\rho_v(r) = \psi_v^2(r)$, the charge components of proton and neutron can be written by

$$\rho_{prot}^e(r) = a_e \rho_s^e(r) + (1 - a_e) \rho_v^e(r) \quad (20)$$

$$\rho_{neut}^e(r) = (1 - a_e) \rho_s^e(r) - a_e \rho_v^e(r), \quad (21)$$

whereas the magnetic components are given by

$$\rho_{prot}^m(r) = a_m \rho_s^m(r) + (1 - a_m) \rho_v^m(r) \quad (22)$$

$$\rho_{neut}^m(r) = (1 - a_m) \rho_s^m(r) + a_m \rho_v^m(r). \quad (23)$$

Mixing terms do not contribute, since $\psi_s(r)\psi_v(r) = 0$.

For the basis states, slope parameters b and (v/c) (with common shape parameter $\kappa = 1.375$ and coupling constant $\alpha = 2.158$), radii and masses are given in **Table 1**, as well as the number of bosons N_g to get similar (absolute) boson and fermion energies. Further, the recoil corrections f'_{rec} were 0.30 and -0.02 for electric binding of scalar and vector states, and 0.26 and 0.14 for magnetic binding, respectively.

Resulting densities and potentials are shown in **Figure 1**. In the upper part the densities are displayed, the boson-exchange and confinement potentials $V_{3g}^{s,v}(r)$ and $V_{2g}^s(r)$ are given in the middle and lower part, respectively. In the middle part the scalar density (rescaled) is shown again by dot-dashed line, which indicates that the geometric condition (5) is really satisfied.

¹ \bar{f} indicating massless fermions (quanta). f is used here instead of q , not to be confused with quarks, massive fermions in quantum chromodynamics.

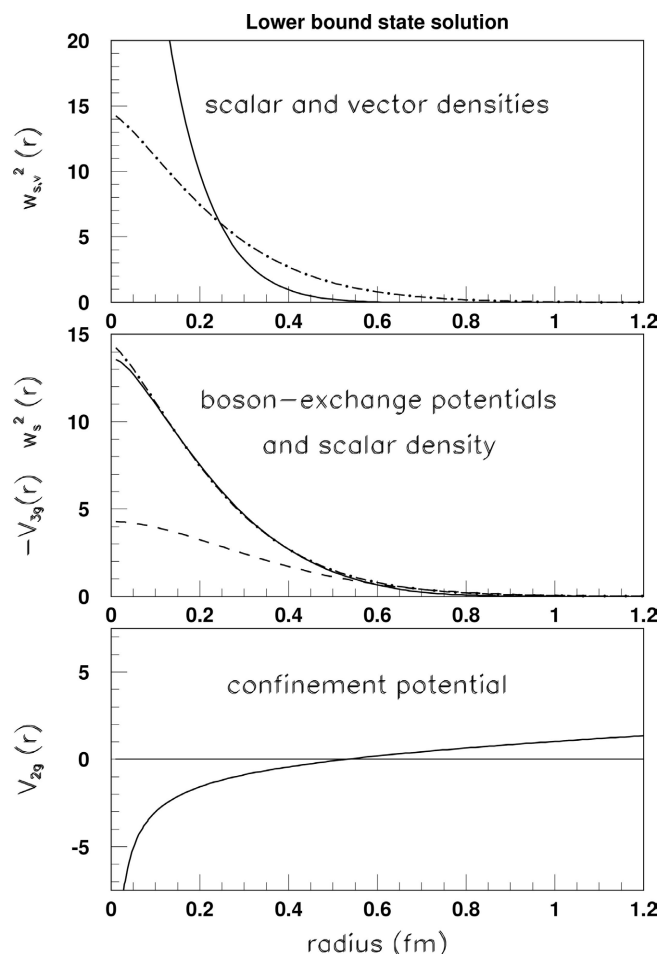


Figure 1. Radial dependence of the densities and potentials of basic bound state solutions. Upper part: Scalar and vector densities $w_s^2(r)$ and $w_v^2(r)$ given by dot-dashed and solid lines. Middle part: Boson-exchange potentials $V_{3g}^{s,v}(r)$ (dashed and solid lines) in comparison with the density $w_s^2(r)$ (dot-dashed line) normalized to the potential $V_{3g}^v(r)$. Lower part: Confinement potential $V_{2g}^s(r)$.

3.1. Deduced Densities, Radii and Magnetic Moments

Concerning the final states, proton and neutron, the condition for a chargeless neutron requires $\int r^2 dr \rho_{neut}(r) = 0$, which yields $a_e = 1/2$. The mixing parameter a_m for magnetic binding was determined mainly from the requirement to get the correct magnetic moments of proton and neutron, which are given by

$$\mathcal{M}_{p,n} = \frac{\langle r_{p,n} \rangle M_{p,n}}{2(\hbar c)(v/c)}, \quad (24)$$

where $\langle r_{p,n} \rangle = \int r^3 dr \psi_{p,n}^2(r) / \int r^2 dr \psi_{p,n}^2(r)$ is the mean linear radius of proton and neutron.

Using $a_m = 0.8228$, the deduced nucleon charge (solid lines) and magnetization densities (dot-dashed lines) are given in **Figure 2**, which show indeed

Table 1. Basis bound state parameters b and (v/c) (with $\kappa = 1.375$ and $\alpha = 2.158$), leading to fermion root mean square radii and masses. The number of bosons is shown in the last column. The slope parameter b and radii are given in fm, the masses in GeV.

type	state	b	$(v/c)^2$	$\langle r_f^2 \rangle^{1/2}$	M_f	N_g
elec	scalar	0.8415	1	0.958	0.957	3×3
"	vector			0.595	1.200	3×5
mag	scalar	0.530	0.35213	0.603	0.806	3×4
"	vector			0.375	1.076	3×6

Table 2. Mixing parameters a_s and a_v , resulting radii, masses and magnetic moments (the radii are given in fm, the masses in GeV).

type	part.	a_s	a_v	$\langle r_f^2 \rangle^{1/2}$	Mass	M_I	$M_{I_{exp}}$
elec	proton	0.5	0.5	0.82 ± 0.02	0.938	-	-
"	neutron	"	"	-	0.940	-	-
mag	proton	0.8228	0.175	0.58 ± 0.02	0.938	2.793	2.793
"	neutron	"	"	0.43 ± 0.02	0.940	1.913	1.913

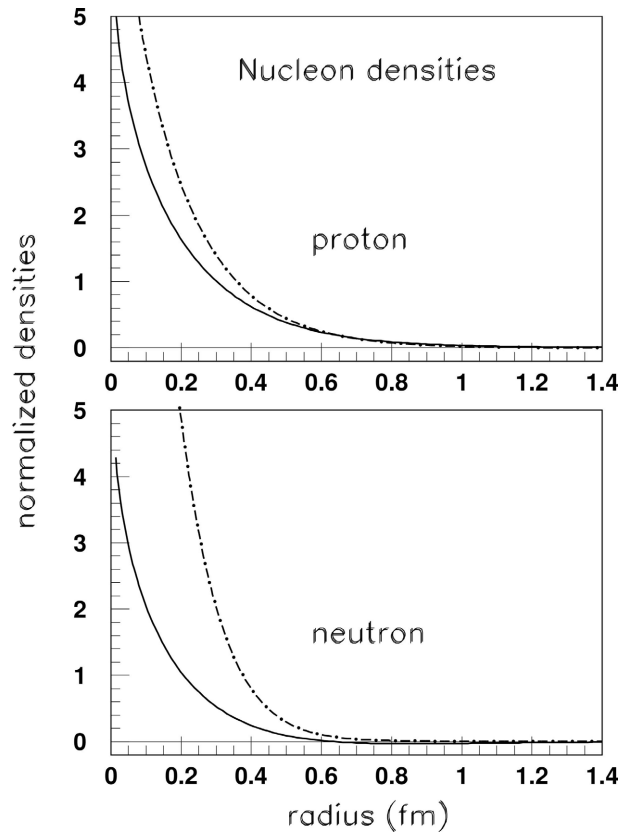


Figure 2. Comparison of the fermion charge and magnetization densities (solid and dot-dashed lines, respectively) for proton and neutron.

significant differences, as found already by Kelly [13]. For the proton these densities are compared with Kelly's empirical analysis in **Figure 3**. Towards the center the present densities increase much stronger than Kelly's results, but in the surface region a reasonable agreement is observed, at least for the charge part. The deduced root mean square radius of 0.82 fm is somewhat smaller than in previous analyses, discussed above. Magnetic binding yields also a quantitative description of the magnetic moments in **Table 2**.

3.2. Masses, the Role of Confinement and Stability

Probably the most important property of nucleons is the large stability—the neutron is slightly heavier than the proton and decays by $n \rightarrow p + e$. Using the binding energies in **Table 1** and writing for electric binding the proton binding energy by $E_b^{elec}(prot) = a_e E_{tot_e}^s + (1 - a_e) E_{tot_e}^v$ and that of the neutron $E_b^{elec}(neut) = (1 - a_e) E_{tot_e}^s - a_e E_{tot_e}^v$, the neutron binding energy turns out to be about -4×10^{-2} GeV, which cannot be correct. By realizing that by changing sign only the contributions from the potentials E_{3g} and ΔE are affected (the other contributions E_{2g} , T_{2g} and T_{1g} are based on derivatives, which do not change sign), we write the fermion binding energies by

$$E^{elec}(prot) = a_e E_{tot_e}^s + (1 - a_e) (E_{3g_e}^v + \Delta E_e^v + E_{2g_e} + T_{2g_e}^v + T_{1g_e}) - f_{stab}^e E_{2g_e}, \quad (25)$$

whereas for the neutron the binding energy is given by

$$E^{elec}(neut) = (1 - a_e) E_{tot_e}^s - a_e (E_{3g_e}^v + \Delta E_e^v - E_{2g_e} - T_{2g_e}^v - T_{1g_e}) + f_{stab}^e E_{2g_e}. \quad (26)$$

At the end of both equations another confinement contribution $f_{stab} E_{2g_e}$ with different sign for proton and neutron is added to get the correct binding energies.

For magnetic binding analogous forms are used

$$E^{mag}(prot) = a_m E_{tot_m}^s + (1 - a_m) (E_{3g_m}^v + \Delta E_m^v + E_{2g_m} + T_{2g_m}^v + T_{1g_m}) + f_{stab}^m E_{2g_m} \quad (27)$$

and

$$E^{mag}(neut) = (1 - a_m) E_{tot_m}^s + a_m (E_{3g_m}^v + \Delta E_m^v + E_{2g_m} + T_{2g_m}^v + T_{1g_m}) - f_{stab}^m E_{2g_m}. \quad (28)$$

Similar expressions have been used for the boson energies, but further adjustment factors $f_{vac}^{e,m}$ are needed. This yields

$$E_g^{elec}(prot) = a_e E_{tot_e}^s + (1 - a_e) (E^{g_e^v} + \Delta E^{g_e} + T^{g_e}) - f_{stabg}^e f_{vac}^e T^{g_e}, \quad (29)$$

$$E_g^{elec}(neut) = (1 - a_e) E_{tot_e}^s - a_e (E^{g_e^v} - \Delta E^{g_e} - T^{g_e}) + f_{stabg}^e f_{vac}^e T^{g_e}, \quad (30)$$

$$E_g^{mag}(prot) = a_m E_{tot_m}^s + (1 - a_m) (E^{g_m^v} + \Delta E^{g_m} + T^{g_m}) + f_{stabg}^m f_{vac}^m T^{g_m}, \quad (31)$$

$$E_g^{mag}(neut) = (1 - a_m) E_{tot_m}^s + a_m (E^{g_m^v} + \Delta E^{g_m} + T^{g_m}) - f_{stabg}^m f_{vac}^m T^{g_m}. \quad (32)$$

Using these formulae (25)-(32), a good fit of the fermion binding energies (the negative of the masses) is obtained with $f_{stab}^e E_{2g_e} = -0.1402$ GeV and $f_{stab}^m E_{2g_m} = -0.0861$ GeV. For bosons the energies are $f_{stabg}^e T^{g_e} = 0.2242$ GeV

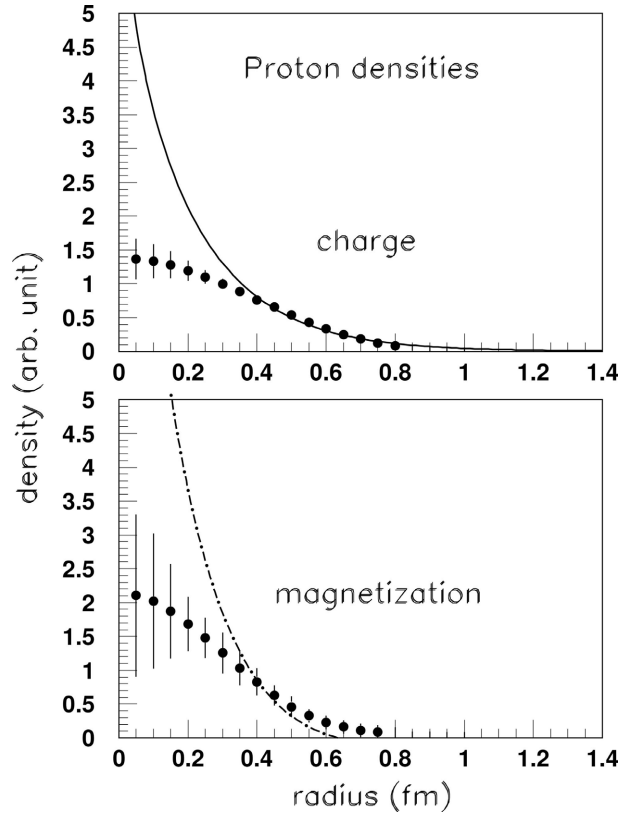


Figure 3. Comparison of the proton charge and magnetization densities with the empirically deduced results of Kelly [13] given by solid points.

and $f_{stab}^m T^{g_m} = 0.0856$ GeV; further $f_{vac}^e = 1.0792$ and $f_{vac}^m = 0.9951$. For a reliable account of the binding energies (nucleon masses), the sum of the adjusted energies $E_{stab} = \sum_{e,m} = f_{stab}^{e,m} E_{2g_{e,m}} + f_{stabg}^{e,m} T^{g_{e,m}}$ should cancel out. However, E_{stab} amounts to 0.0835 GeV (9% of the nucleon mass), which is not very satisfactory.

Table 3. Excess energies $f_{stab}^{e,m} E_{2g_{e,m}}$, $f_{stabg}^{e,m} T^{g_{e,m}}$ and vacuum energies $E^{e,m}(V_o)$ (in GeV) for electric and magnetic binding, leading to a sum of all six contributions $E_{stab}^{tot} = 0$. In the last column a comparison of $E^{e,m}(V_o)$ with vacuum energies $2E_{elec}(V_o)$ calculated from the binding of electrons [Mo2] (enhanced by 12%).

type	$f_{stab} E_{2g}$	$f_{stabg} T^g$	$E(V_o)$	$2E_{elec}(V_o)$
elec	-0.1402	0.2242	-0.0669	-0.067
mag	-0.0861	0.0856	-0.0166	-0.017

Since the fermion confinement potential (7) includes a small constant V_o , which does not exist in the boson part, the extra factors f_{vac}^e and f_{vac}^m can be related to a (vacuum) energy $E(V_o)$. Using $E^{e,m}(V_o) \sim E_{2g_{e,m}} |f_{vac}^{e,m} - 1|$, this leads to $E^{e,m}(V_o)$ of -0.0669 GeV and -0.0166 GeV, respectively. Adding $E^{e,m}(V_o)$ to E_{stab} yields 0.0835 GeV, which satisfies indeed $E_{stab}^{tot} = E_{stab} + E^{e,m}(V_o) = 0$.

These results are summarized in **Table 3**.

Interestingly, if we assume that $E(V_o)$ scales with the mass of the particle, we obtain already from binding of the electron with $E_{elec}(V_o)$ of -0.202×10^{-5} GeV [Mo2] for the nucleon a vacuum energy for electric and magnetic binding $E^e(V_o) + E^m(V_o)$ of -0.0748 GeV (this value is already multiplied by 2, since we deal with 2 particles, proton and neutron). If we take further a value of $E_{elec}(V_o)$ 12% larger (which is certainly within the parameter uncertainties of the electron analysis [Mo2]) and assume that the vacuum energies $E^e(V_o)$ and $E^m(V_o)$ are related to the average volume $(4\pi/3)\bar{R}_{e,m}^3$ of these bound states (where $\bar{R}_{e,m}$ are their average root mean square radii), we obtain values of $E^{e,m}(V_o)$ of -0.067 GeV and -0.017 GeV, which are very similar to the extracted vacuum energies, as shown in the last column of **Table 3**.

Finally, electric binding has the largest excess energy, see **Table 3**, negative for proton and positive for neutron. The stronger extra binding of the proton together with a more compact momentum distribution (smaller root mean square momentum) indicates that a free neutron can decay to a proton by emitting an electron $n \rightarrow p + e$.

3.3. Electromagnetic form Factor Ratios

The Fourier transformed densities in momentum space can be related to the electromagnetic form factors $G_E(q)$ and $G_M(q)$ multiplied with the magnetic moments. However, these form factors have large experimental uncertainties. Therefore, form factor ratios are usually plotted, in which the errors are strongly reduced. This yields

$$\mu_p G_{Ep}(q)/G_{Mp}(q) = [a_e \rho_s^e(q) + (1-a_e) \rho_v^e(q)] / [a_m \rho_s^m(q) + (1-a_m) \rho_v^m(q)] \quad (33)$$

and

$$\mu_n G_{En}(q)/G_{Mn}(q) = [a_e \rho_s^e(q) - (1-a_e) \rho_v^e(q)] / [a_m \rho_s^m(q) - (1-a_m) \rho_v^m(q)]. \quad (34)$$

Since the scalar state is assumed of $3(f \bar{f})f$ structure, the energy is increased by the same factor 3 with respect to a $(f \bar{f})f$ state. Also for the average momentum and the Fourier transformed densities $\rho_x(q) = 4\pi \int r^2 dr j_o(qr) \rho_x(r)$ this is needed, where $j_o(qr)$ is now given by $j_o(qr) = \sin(3qr)/(3qr)$. The results are shown in **Figure 4** by solid lines in comparison with a selection of experimental data [14] [15]. For the proton this confirms quite well the experimental fall off of the form factor ratio at small momentum transfers. However, at larger momenta the deduced data points fall off definitively too much. This can be proven by showing $G_{Ep}(q)$ only (dashed-dotted line), which falls off quite similar to the data points. However, if this curve is divided by $G_{Em}(q)/\mu_p$ (which falls off also), the form factor ratio increases up to the solid line. This default of the experimental data points could be due to efficiency problems or to background overestimations in the rather complex data analysis. For the

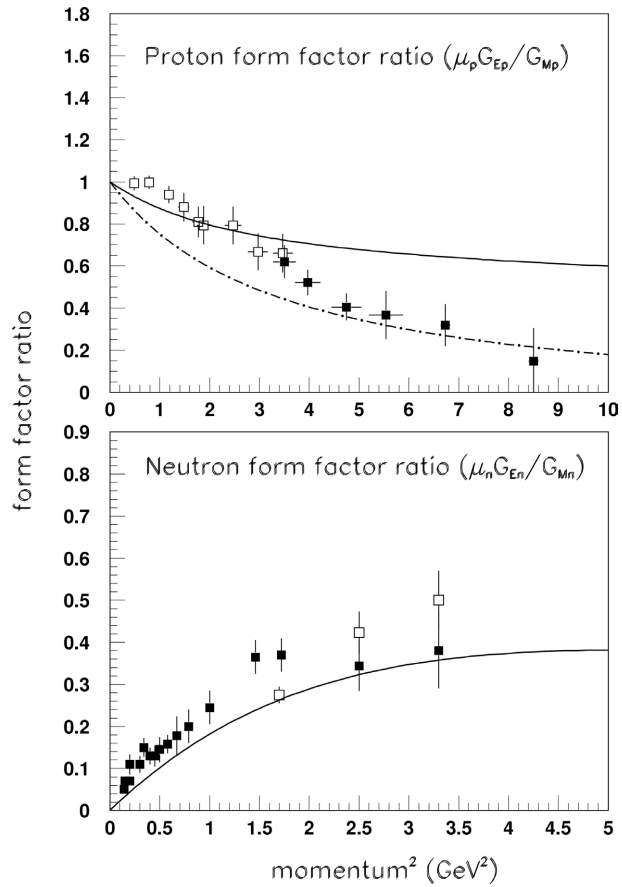


Figure 4. Selection of electromagnetic form factor ratios $\mu G_E / G_M$ for proton and neutron from refs. [14] [15] (the open and closed points show data samples from different experiment analyses) in comparison with our results. Upper part: Experimental data on the proton in comparison with calculated form factor ratio (the dashed line shows the electric form factor G_{E_p} only). Lower part: Same for the neutron.

neutron the agreement of the momentum dependence between experimental form factor ratio and our calculation is better. Still, the data points are somewhat larger, indicative of a larger background contribution.

4. Conclusions

The analysis of nucleons in a bound state formalism based on a fermion-boson symmetric Lagrangian has shown that a quantitative description of important nucleon properties could be achieved, assuming a mixing of a $3 \cdot (f \bar{f}) f$ state with scalar coupling between its constituents with a corresponding $(f \bar{f}) f$ bound state of vector coupling. All basic parameters are constrained by boundary conditions on energy and momentum conservation; further, two mixing parameters are adjusted to get neutron charge neutrality and the correct magnetic moments of proton and neutron. The mixing of these basic states gives rise to quite different proton and neutron density distributions, first observed by Kelly but not really

understood up to present.

Of particular interest is the high stability of the nucleon. Responsible for this property is the dynamically generated confinement potential (and the related second order boson potential), giving rise to negative/positive *extra* energies for electric binding of the proton/neutron and opposite for magnetic binding of these particles. This indicates that binding and repulsion (electric and magnetic) is present at the same time for both particles, which blocks the decay of these particles. Further, the detailed extra binding is different for both particles, which allows decay of the neutron to proton and electron. Small vacuum energies are present to get complete cancellation of all terms. This shows a rather complex mixing of the different components, very different from the binding of leptons, in which just a cancellation of the fermion and boson energies takes place.

Confinement has been indeed expected as the origin of the high stability of the proton in many empirical pictures, where it is expected to provide an attractive flux tube in extensions of the constituent quark model or leads to stable string tensions in higher dimensional string models.

Other systems as “strange” baryons Σ^\pm and Λ may have a structure similar to nucleons. Thus, it would be interesting to see, whether these particles can be understood in a similar way and why these particles are not stable.

Acknowledgements

I am grateful to several colleagues, in particular to Benoit Loiseau for his help to establish details of the theory and to Thomas Seifick for setting up the Web-presentation <https://h2909473.stratoserver.com> for on-line calculations of leptons and mesons.

Conflicts of Interest

The author declares no conflicts of interest regarding the publication of this paper.

References

- [1] Hofstadter, R. (2016) The Electron-Scattering Method and Its Application to the Structure of Nuclei and Nucleons. *Nobel Lecture 1961—Electromagnetic form Factors of the Proton*, Stockholm.
- [2] Jones, M.K., *et al.* (2000) G_{E_p}/G_{M_p} Ratio by Polarization Transfer in $ep \rightarrow ep$. *Physical Review Letters*, **84**, 1398.
- [3] Gayou, O., *et al.* (2002) Measurement of G_{E_p}/G_{M_p} in $ep \rightarrow ep$ to $Q^2 = 5.6 \text{ GeV}^2$. *Physical Review Letters*, **88**, Article ID: 092301.
- [4] Punjabi, V., *et al.* (2005) Proton Elastic form Factor Ratios to $Q^2 = 3.5 \text{ GeV}^2$ by polarization transfer. *Physical Review C*, **71**, Article ID: 055202.
- [5] Puckett, A.J.R., *et al.* (2002) Recoil Polarization Measurements of the Proton Electromagnetic Form Factor Ratio to $Q^2 = 8.5 \text{ GeV}^2$. *Physical Review Letters*, **104**, Article ID: 242301.
- [6] Puckett, A.J.R., *et al.* (2012) Final Analysis of Proton form Factor Ratio Data at $Q^2 = 4.0, 4.8, \text{ and } 5.6 \text{ GeV}^2$. *Physical Review C*, **85**, Article ID: 045203.

- [7] Liyanage, A., *et al.* (2020) Proton Form Factor Ratio $\mu_p G_E^p / G_M^p$ from Double Spin Asymmetry. *Physical Review C*, **101**, Article ID: 035206.
- [8] Madey, R., *et al.* (2002) Measurements of G_E^n / G_M^n from the ${}^2\text{H}(\mathbf{e}, \mathbf{e}'\mathbf{n}){}^1\text{H}$ Reaction to $Q^2 = 1.45(\text{GeV}/c)^2$. *Physical Review Letters*, **91**, Article ID: 122002.
- [9] Bradford, R., Bodek, A., Budd, H. and Arrington, J. (2006) A New Parameterization of the Nucleon Elastic Form Factors. *Nuclear Physics B—Proceedings Supplements*, **159**, 127-132. <https://doi.org/10.1016/j.nuclphysbps.2006.08.028>
- [10] Geis, E., *et al.* (2008) Charge Form Factor of the Neutron at Low Momentum Transfer from the ${}^2\text{H}(\mathbf{e}, \mathbf{e}'\mathbf{n}){}^1\text{H}$ Reaction. *Physical Review Letters*, **101**, Article ID: 042501.
- [11] Riordan, S., *et al.* (2010) Measurements of the Electric Form Factor of the Neutron up to $Q^2 = 3.4 \text{ GeV}^2$ Using the Reaction ${}^3\text{He}(\mathbf{e}, \mathbf{e}'\mathbf{n})pp$. *Physical Review Letters*, **105**, Article ID: 262302.
- [12] Mohr, P.J., Taylor, B.N. and Newell, D.B. (2012) CODATA Recommended Values of the Fundamental Physical Constants: 2010. *Reviews of Modern Physics*, **84**, 1527-1605. <https://doi.org/10.1103/revmodphys.84.1527>
- [13] Kelly, J.J. (2002) Nucleon Charge and Magnetization Densities from Sachs Form Factors. *Physical Review C*, **66**, Article ID: 065203. <https://doi.org/10.1103/physrevc.66.065203>
- [14] Punjabi, V. (2012) Nucleon form Factors, Jlab Users Group Meeting, Jefferson Lab, Newport News, with a Discussion of Data of Refs.
- [15] Arrington, J. (2015) Overview of Proton, Neutron, and Pion form Factor Measurements. QCD Bound States Workshop, Argonne National Lab.
- [16] Capstick, S. and Isgur, N. (1986) Baryons in a Relativized Quark Model with Chromodynamics. *Physical Review D*, **34**, 2809-2835. <https://doi.org/10.1103/physrevd.34.2809>
- [17] Simonov, Y.A. (2003) Nonperturbative Quark Dynamics in a Baryon. arXiv: hep-ph/0205334.
- [18] Thomas, A.W., Théberge, S. and Miller, G.A. (1981) Cloudy Bag Model of the Nucleon. *Physical Review D*, **24**, 216-229. <https://doi.org/10.1103/physrevd.24.216>
- [19] Hosaka, A. and Toki, H. (1996) Chiral Bag Model for the Nucleon. *Physics Reports*, **277**, 65-188. [https://doi.org/10.1016/s0370-1573\(96\)00013-0](https://doi.org/10.1016/s0370-1573(96)00013-0)
- [20] Nakamura, K. (2010) Review of Particle Physics. *Journal of Physics G: Nuclear and Particle Physics*, **37**, Article ID: 075021. <https://doi.org/10.1088/0954-3899/37/7a/075021>
- [21] Roberts, C.D. and Williams, A.G. (1994) Dyson-Schwinger Equations and Their Application to Hadronic Physics. *Progress in Particle and Nuclear Physics*, **33**, 477-575. [https://doi.org/10.1016/0146-6410\(94\)90049-3](https://doi.org/10.1016/0146-6410(94)90049-3)
- [22] Barbieri, R., Kögerler, R., Kunszt, Z. and Gatto, R. (1976) Meson Masses and Widths in a Gauge Theory with Linear Binding Potential. *Nuclear Physics B*, **105**, 125-138. [https://doi.org/10.1016/0550-3213\(76\)90064-x](https://doi.org/10.1016/0550-3213(76)90064-x)
- [23] Eichten, E., Gottfried, K., Kinoshita, T., Lane, K.D. and Yan, T. (1978) Charmonium: The Model. *Physical Review D*, **17**, 3090-3117. <https://doi.org/10.1103/physrevd.17.3090>
- [24] Ebert, D., Faustov, R.N. and Galkin, V.O. (2003) Properties of Heavy Quarkonia and B_c Mesons in the Relativistic Quark Model. *Physical Review D*, **67**, Article ID: 014027. <https://doi.org/10.1103/physrevd.67.014027>
- [25] Isgur, N. and Paton, J. (1985) Flux-Tube Model for Hadrons in QCD. *Physical Review*

- D*, **31**, 2910-2929. <https://doi.org/10.1103/physrevd.31.2910>
- [26] Barnes, T., Close, F.E. and Swanson, E.S. (1995) Hybrid and Conventional Mesons in the Flux Tube Model: Numerical Studies and Their Phenomenological Implications. *Physical Review D*, **52**, 5242-5256. <https://doi.org/10.1103/physrevd.52.5242>
- [27] Tan, Z.G., Mo, Y.F. and Sun, L.P. (2019) Structure of Proton Based on the Classical String Model. arXiv: 1908.01307.
- [28] Carlson, C.E. and Vanderhaeghen, M. (2008) Empirical Transverse Charge Densities in the Nucleon and the Nucleon-To- δ Transition. *Physical Review Letters*, **100**, Article ID: 032004. <https://doi.org/10.1103/physrevlett.100.032004>

References to Own Work

- [MSD] H.P. Morsch, W. Spang and P. Decowski, Folding study of α -p scattering: Systematics of elastic scattering, effective interaction and inelastic excitation of N^* resonances, *Phys. Rev.* **67**, 064001 (2003)
- [Mo1] H.P. Morsch, Acceleration in a fundamental bound state theory and the fate of gravitational systems, *J. Adv. Math. and Comp. Sc.* **28**(3): 1-13 (2018)
- [Mo2] H.P. Morsch, Bound state description of particles from a quantum field theory of fermions and bosons, compatible with relativity, *J. High Energy Physics, Gravity and Cosmology* **10**, 562 (2024)
- [Mo3] H.P. Morsch, Unique structure of particle bound states, *Brit. J. Math. and Comp. Sc.* **17**(6): 1-11 (2016)
- [Mo4] H.P. Morsch, Fundamental bound state description of light atoms and the fine structure constant $\alpha \sim 1/137$, *Boson J. Modern Phys.* **3**,1: 197 (2017)
- [Mo5] H.P. Morsch, Lepton bound state theory based on first principles, *J. Adv. Math. and Comp. Sc.* **36**(3): 118 (2021)
- [Mo6] H.P. Morsch, Origin of gravitation and description of galaxy rotation in a fundamental bound state approach, *Global J. Sci. Front. Research. A* **18**, 4 v.1, p. 25 (2018)